EFFECTS OF ENTRAINED AIR ON THE PERFORMANCE OF CENTRIFUGAL AND AXIAL FLOW PUMPS

MITSUKIYO MURAKAMI and KIYOSHI MINEMURA

Department of Mechanical Engineering

HAKARU SUEHIRO

Toyota College of Technology, Toyota, Aichi

(Received June 4, 1971)

1. Introduction

Entrained air in centrifugal pumps has undesirable effects on their performance and the attention is paied to prevent the air admission. In practical use, however, air is drawn into the pumps through inadiquate stuffing boxes or loose fittings of suction pipes. In some cases, air entrainment will be brought about due to a vortex formation in a suction well or by separation of air bubbles contained in pumping medium, such as pulp or slurry. Head and capacity of pumps are reduced continously as the air volume referred to the suction pressure is increased, until the pumps lose prime. The allowable maximum of air volume with which the pumps can keep operation is varied by the types of pumps, but the volume is, in general, within several percentages of the discharging water (in the extreme case it attains to 15%).

In the past[1)2)3)], some papers on these problems have been published, but systematic data on the behaviour of entrained air in pump impellers and investigations of its effects on the pump performance are required.

In this paper, movement of the entrained air bubbles in a pump impeller was observed by employing a semi-open impeller pump with a transarent casing (pump II in Table 1) and the effects of air on the pump performances were studied. The effects of air were also compared for three different types of pumps.

Nomenclature

A_2 = discharging area of impeller outlet
d = diameter of throttle orifice
D = diameter of suction pipe
g = acceleration of gravity
H = head of pump in meter of pure water
H_c = head of pump in meter of air-water mixture
N = number of revolutions per minute
q_s = flow volume of entrained air referred to suction pressure
Q = flow volume of water
u_2 = peripheral speed of impeller outlet
γ_w = specific weight of water

γ_a = specific weight of air
γ_{a+w} = specific weight of air-water mixture
Φ = capacity coefficient, Q/A_2u_2
Ψ = head coefficient, $H_c/(u_2^2/g)$
η_p = pump efficiency
δ = diameter of air bubble

2. Experimental Apparatus and Measurements

A schematic diagram of the experimental apparatus and the specifications of the pumps employed are shown in Fig. 1 and Table 1, respectively. The volume of pumping water was determined by means of a metering tank for the pump I, a weir for the pump II, and an inlet nozzle for the pump III, respectively. To measure the water quantities when the pumps lost prime, elbow meters were installed in the suction pipes. Air was introduced into the suction pipes through various openings as shown in Fig. 2, and the air volume was measured by orifices. To clarify the effects of size and location of the air inlet, two different air pipes of diameters 6 and 16 mm, and air openings with several holes (diameter = 1.5 mm) were employed at different sections of the pipes. Suction pressures of

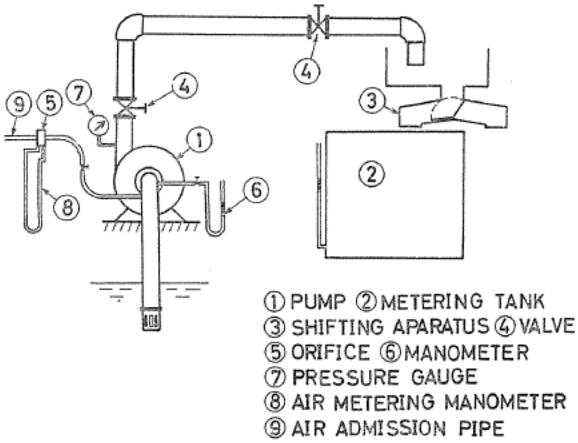

FIG. 1. Arrangement of experimental apparatus.

TABLE 1. Pumps employed in this experiment

No.	Types of pumps	Diameter of suction pipe (mm)	R.P.M.	Q (m^3/s)	H (m)	Specific speed
I	two-stage centrifugal type	130	1750	2.0	48	136
II	single-stage centrifugal type	60	1750	0.6	18	155
III	axial flow type	250	1350	6.5	4	1217

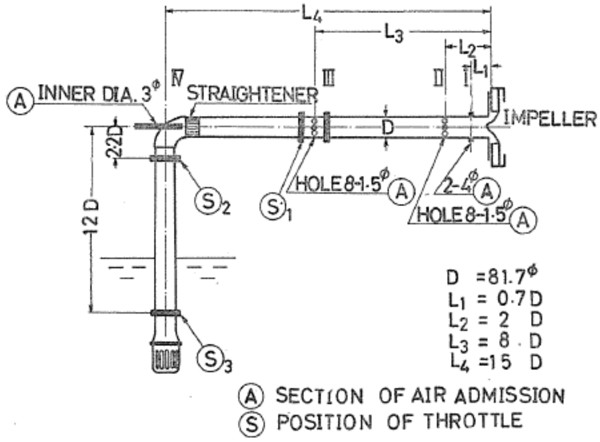

FIG. 2. Position of air admitting ports and throttle plates.

pumps were changed by adjusting the water level in a suction well (pumps I and III) and setting throttle plates in the suction pipe (pump II). The throttle ratios of the orifices d/D were 0.50 and 0.75.

3. Equations to Predict Experimental Results

The performance of pumps when air is entrained, is conveniently expressed by the weights of the air and water mixture. The specific weight of the mixture is given by

$$\gamma_{a+w} = (Q\gamma_w + q\gamma_a)/(Q+q) \tag{1}$$

Within the operating range of pumps the weight of air is only a fraction of that of water and $q\gamma_a \ll Q\gamma_w$, and hence, Eq. (1) gives

$$\gamma_{a+w} \fallingdotseq \gamma_w\{1-(q/Q)\} \tag{2}$$

Thus, the corrected head referred to the mixture is

$$H_c = (\gamma_w/\gamma_{a+w})H \tag{3}$$

4. Pump Performances

4.1. Effects of Air Volume for Different Pump Speeds

Fig. 3 shows $\Psi-\Phi$ curves of pump I for three different speeds. Within the range of small air volume, the pump head Ψ is reduced gradually as the air volume increases, which satisfies affinity laws, except the extreme capacities. Reduction of capacities due to air admission is remarkable at greater capacities, where each speed gives different curves. This will be attributable to the occurence of cavitation in pump impellers. At low capacities, the pump loses prime with a little air volume. Fig. 4 shows the relationship between $\Psi/\Psi_{\max}$ and $\Phi/\Phi_{\max}$, where $\Psi_{\max}$ and $\Phi_{\max}$ refer to the maximum values of Ψ and Φ for

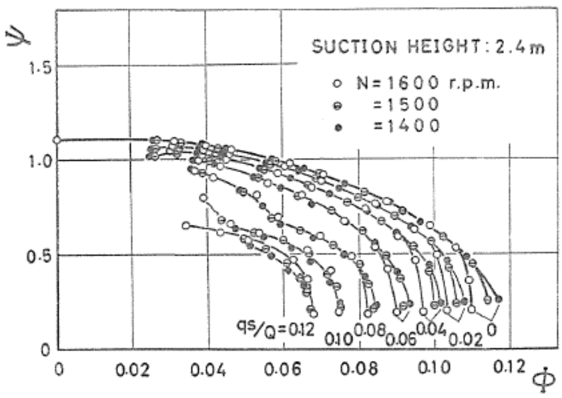

FIG. 3. Change of head, Ψ-capacity, Φ curves due to air admission, (pump I).

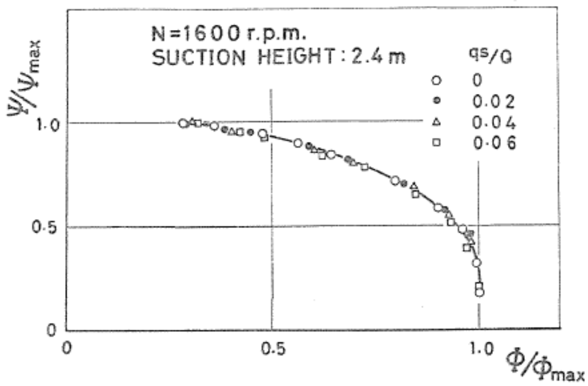

FIG. 4. $\Psi/\Psi_{max}-\Phi/\Phi_{max}$ curve.

each air ratio, respectively. The relationships can be expressed by a single curve and hence, the capacity Φ–head Ψ curves for any air-water mixture can be drawn from the results of pure water within the range of $q_s/Q \leqq 0.06$. Figs. 5 and 6 are performance curves for the pumps II and III, respectively. The similar relationships are also obtained.

Fig. 7 reveals the maximum volume of allowable air against the pump capacity for the pump I. Each curve has its maximum and it is seen that much air can be delivered by the impeller having higher speeds. This will probably be attributable to the fact that the impeller with a higher speed has higher flow velocity for the same capacity Φ and higher capability for air delivering. In addition, air is broken into finer bubbles by an impeller with higher speeds as is described later, resulting in also higher capacity of air delivering. The maximum amount of the allowable air is changed by the difference of pump types. Fig. 8 is the results for the pump III. Each curve has a minimum point, where some unsteady flows are developed in the impeller. The radial flow pump II has also nearly the same tendency.

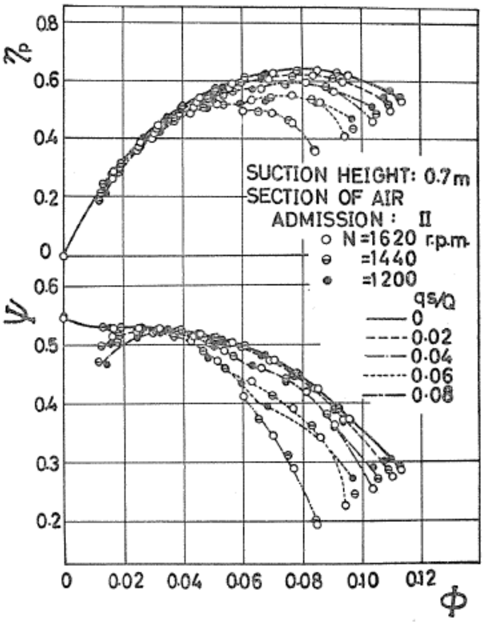

FIG. 5. Performance curves for pump II.

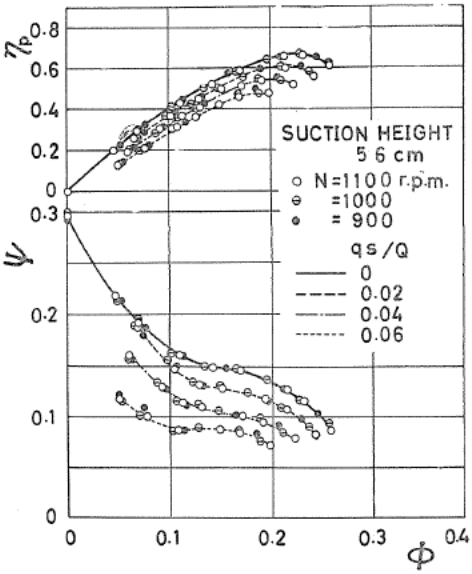

FIG. 6. Performance curves for pump III.

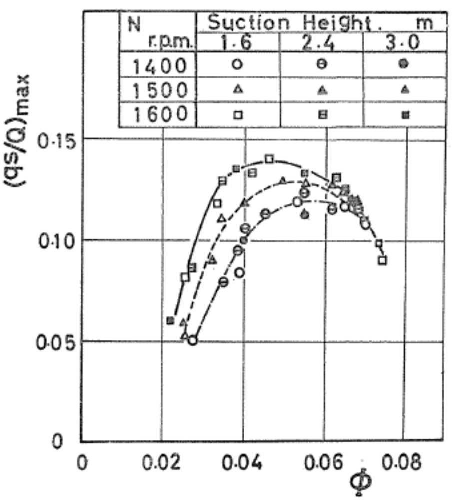

FIG. 7. The maximum allowable air for pump I.

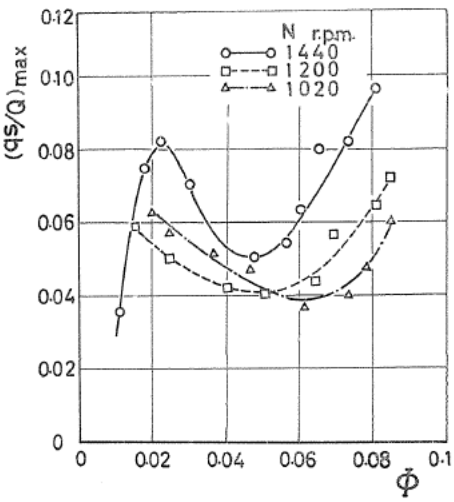

FIG. 8. The maximum allowable air for pump III.

4.2. Effects of Location and Size of Air Openings

Fig. 9 shows the influence of location and size of the ports admitting air on the performance of pump II. Difference of the size and location of the ports has a slight effect on the performance. When $q_s/Q>0.04$, discontinuities of the curves appear. To investigate the discontinuities, air was admitted to the suction

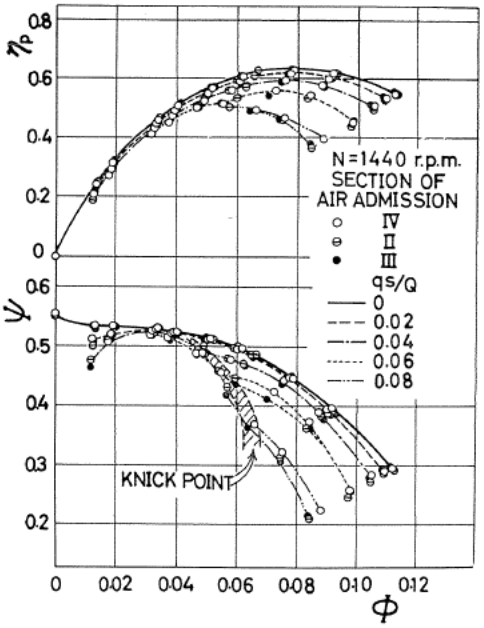

FIG. 9. Influences of location and size of air admitting ports, (pump II).

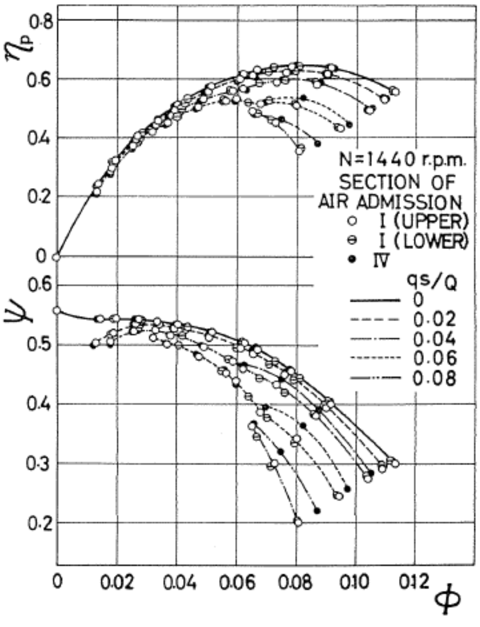

FIG. 10. Discontinuities of performance curves, (pump II).

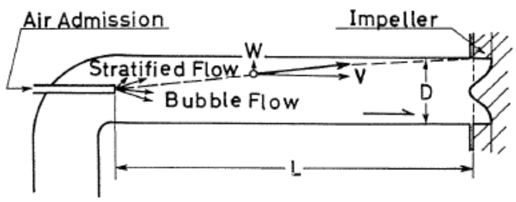

FIG. 11. Flow patterns of entrained air in a suction pipe.

pipe at two sections I and IV in Fig. 2, and the performance was tested. The results are shown in Fig. 10. The curves with air admission at section IV have much remarkable discontinuities. At a smaller capacity than $\Phi=0.05$, water velocity in the suction pipe is very slow and the air admitted from section IV rises to the top of the pipe as is seen in Fig. 11. In this condition, the air enters the impeller in a state of layer. However, when $\Phi>0.05$, the air enters it in a nearly uniformly distributed state. When air is admitted to the top of the section I, it enters the impeller without dispersion, but when air is admitted to the bottom of the same section, it enters uniformly the impeller. In both cases, the diameter of air bubbles is larger than 2 mm. The air in the suction pipe is broken by the fast moving impeller into fine bubbles and the bubble diameters in the impeller are nearly uniform, ranging from 0.2 to 0.4 mm. The mean values decrease as the pump speed increases, Fig. 18. Thus, the difference of flow patterns of air in the suction pipes has a little effect on the flow picture in the impeller, except when the pump is operating near the critical conditions

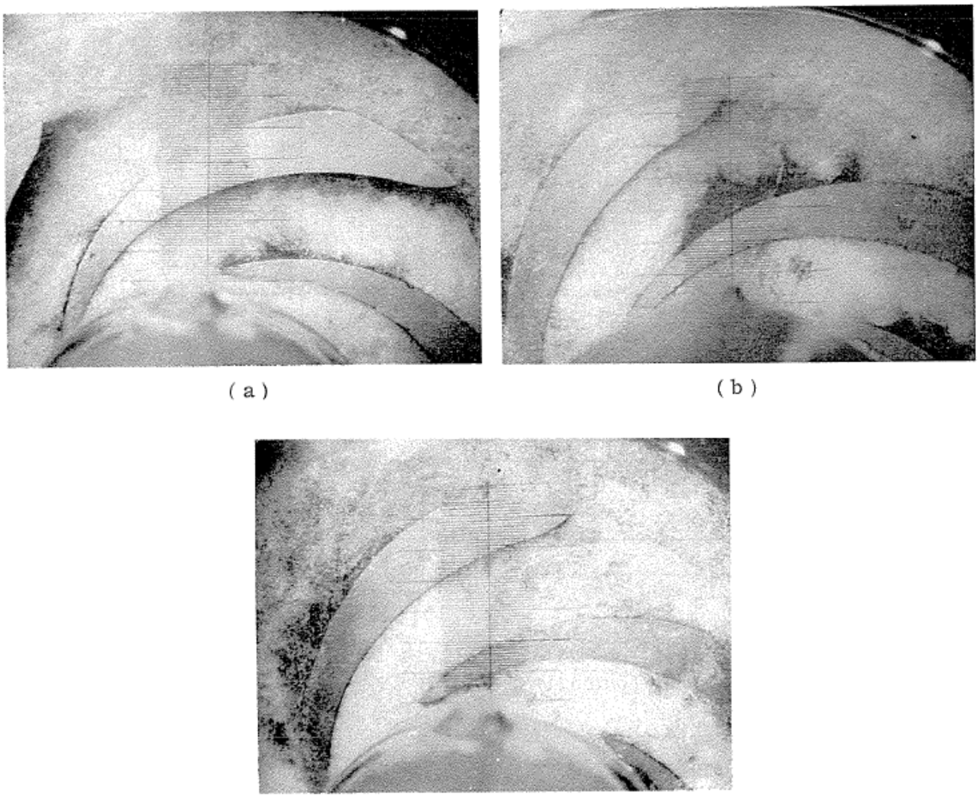

(a) (b) (c)

FIG. 12. Photographs of air flow in the impeller channels of pump II.
(a), (c): uniform flows of air bubbles.
(b): non-uniform flows of air bubbles.

of prime. In these conditions, discontinuities appear on the performance curves due to a change of flow patterns in the impeller, which corresponds to the flow change in the suction pipes. At these discontinuities, the flow conditions of air in the impeller change intermittently as shown in Fig. 12 (b), where the air bubbles are seen to be white, and the black space exhibits the pure water region. The pictures (a) and (c) in this figure show uniform and steady conditions of air flow in the impeller channels.

4.3. Effects of Suction Pressure

Fig. 13 shows the effects of suction height or pressure on the performance of the pump I, and its available NPSH for various suction heights is given in Fig. 14. The performance curves for different suction heights are brought in a single curve, except the region near the maximum capacities, where cavitation grows. By changing the suction pressure with throttle plates, the performance of pump II is also tested, Fig. 15. The available NPSH is also shown in Fig. 16. Any appreciable change of the performance can not be seen in the range of small air ratio $q_s/Q<0.06$.

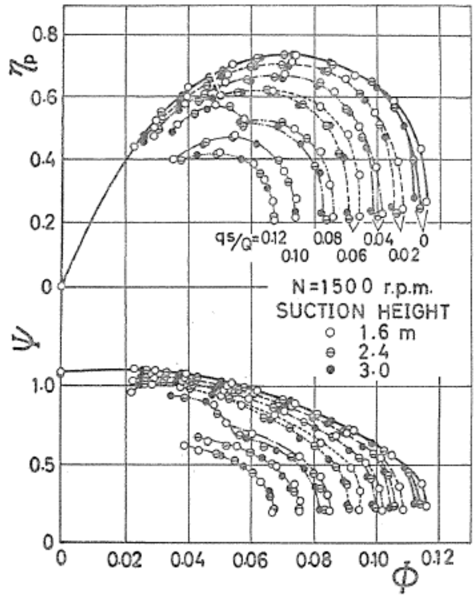

FIG. 13

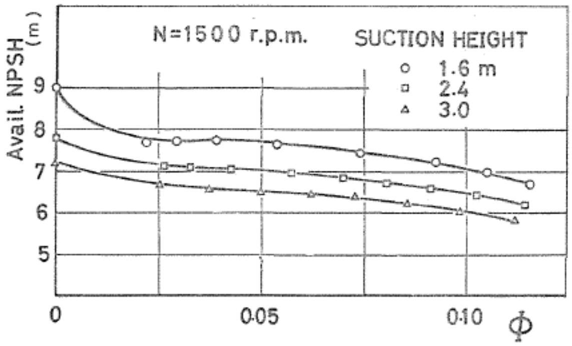

FIG. 14

FIG. 13. Effects of suction heights on the performance of pump I.

FIG. 14. Available NPSH of pump I.

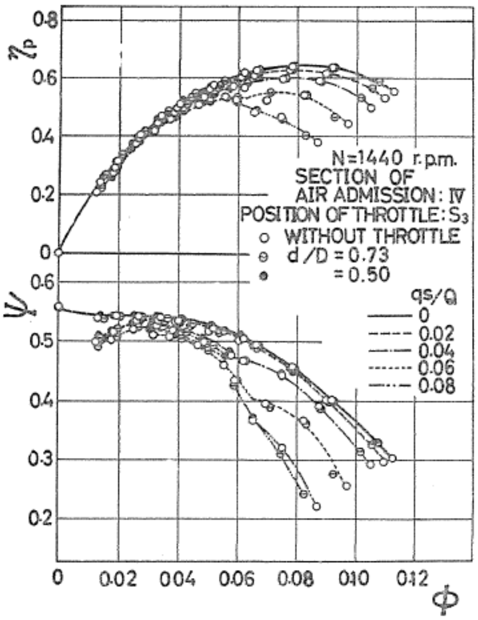

FIG. 15

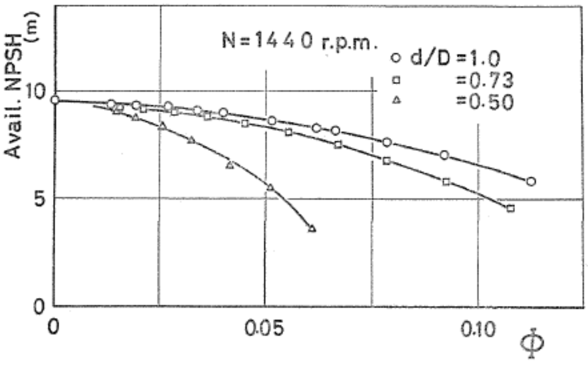

FIG. 16

FIG. 15. Effects of suction pressures on the performance of pump II.

FIG. 16. Available NPSH of pump II.

5. Flow of Air in Pump Impellers

As mentioned already, size and flow patterns of air bubbles in the suction pipes are influenced remarkably by the pump capacities and the location of air

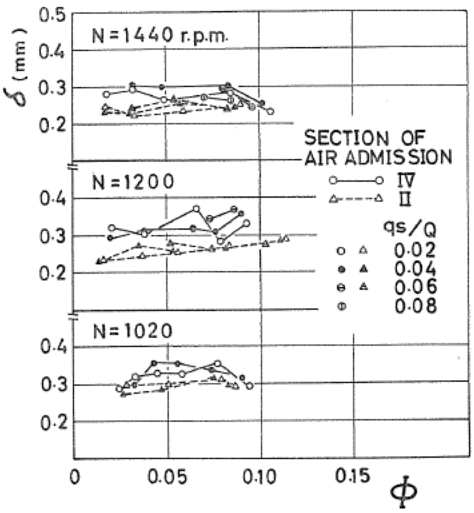

FIG. 18

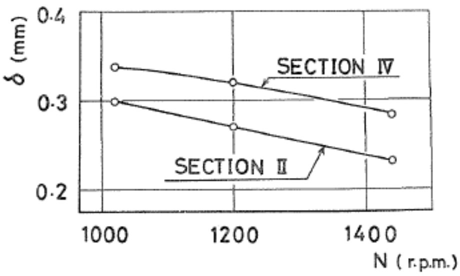

FIG. 17

FIG. 17. Change of bubble diameters in the impeller of pump II.

FIG. 18. Relations of bubble diameters against pump speeds, (pump II).

admission. However, the air is crashed by the impeller into fine pieces of nearly uniform size. The size can be measured in the photographs as shown in Fig. 12. An example of the results is given in Fig. 17. A considerable divergence of the diameters is seen for each speed, but no appreciable difference can be observed for different values of Φ and q_s/Q. The diameter ranges from 0.2 to 0.4 mm, depending on the location of air admitting ports and on pump speeds. The diameter diminishes as the speed increases, Fig. 18. Change of bubble diameters between the inlet and outlet sections of the impeller can not be discriminated, despite the presence of a considerable pressure difference, which may deserve further investigations.

6. Conclusion

1. Within the range of $q_s/Q < 0.04 \sim 0.06$, the performances of centrifugal and axial flow pumps are reduced continuously as the entrained air increases. The performance curves are changed with nearly similar profiles. The change of performance is generally expressed by a parameter q_s/Q, irrespective of sunction pressures or pump speeds.

2. The pumps lose prime when q_s/Q exceeds $0.07 \sim 0.15$, which depends on the pump types.

3. The maximum value of q_s/Q with which the pumps can keep continual operation is reached at a certain pump capacity, and the value increases as the pump speeds.

4. The flow conditions of air bubbles entrained in suction pipes are largely changed by the location and manner of air entrainment. The air is broken by pump impellers into nearly uniform bubbles and the mean diameter of the bubbles in the impellers is the order of 0.3 mm, which decreases as the pump speeds increase.

References

1) W. Siebrecht, V. D. I., 74, 3, (1930), 87.
2) A. J. Stepanoff, Centrifugal and Axial Flow Pumps, 2nd Ed., (1957), 230, Hohn Wiley and Sons, INC.
3) M. Murakami *et al.*, Proceedings of 13th Congress of the International Association for Hydraulic Research, Vol. 2, (Subject B), (1969), 71.